LETTER

Self-Cleaning CO_2 Reduction Systems: Unsteady Electrochemical Forcing Enables Stability

Yi Xu, Jonathan P. Edwards, Shijie Liu, Rui Kai Miao, Jianan Erick Huang, Christine M. Gabardo, Colin P. O'Brien, Jun Li, Edward H. Sargent,* and David Sinton*

Read Online

ACCESS | Metrics & More | Article Recommendations | Supporting Information

ABSTRACT: The electrochemical conversion of CO_2 produces valuable chemicals and fuels. However, operating at high reaction rates produces locally alkaline conditions that convert reactant CO_2 into cell-damaging carbonate salts. These salts precipitate in the porous cathode structure, block CO_2 transport, reduce reaction efficiency, and render CO_2 electrolysis inherently unstable. We propose a self-cleaning CO_2 reduction strategy with short, periodic reductions in applied voltage, which avoids saturation and prevents carbonate salt formation. We demonstrate this approach in a membrane electrode assembly (MEA) with silver and copper catalysts, on carbon and polytetrafluoroethylene (PTFE)-based gas diffusion electrodes, respectively. When operated continuously, the C_2 selectivity of the copper−PTFE system started to decline rapidly after only ∼10 h. With the self-cleaning strategy, the same electrode operated for 157 h (236 h total duration), maintaining 80% C_2 product selectivity and 138 mA cm^{-2} of C_2 partial current density, at a cost of <1% additional energy input.
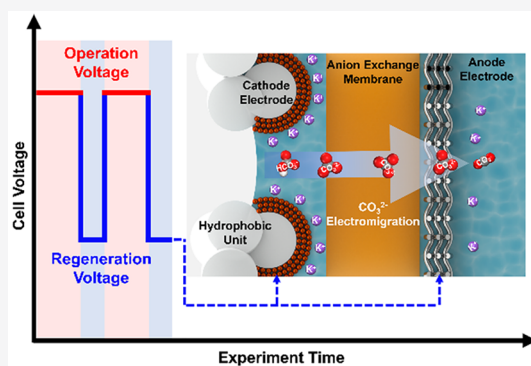
The reduction of carbon dioxide (CO_2) emissions is essential to mitigate climate change-driven environmental damage.[1,2] The rapidly decreasing cost of renewable electricity, coupled with the need for energy storage from these intermittent sources,[3−7] has motivated electrochemical pathways for the CO_2 reduction reaction (CO_2RR) to valuable chemicals and fuels.[8−12]

Gas diffusion electrodes facilitate effective CO_2 mass transport to the cathode catalyst (Figure 1a),[13] enabling electrolyzers to operate at the current densities required for industrial deployment, *e.g.*, in excess of 100 mA cm^{-2}.[14,15] Alkali metal cations, typically potassium, are implemented broadly in aqueous electrolytes to reduce ohmic losses and improve the CO_2RR current density and selectivity.[16,17] Performing CO_2 electrolysis at high current densities inevitably produces large quantities of hydroxide ions on the cathode, driving up the local pH and thus encouraging the chemical reaction of dissolved CO_2 with these hydroxide ions to produce bicarbonate ions on route to carbonate ions (Figure 1b).[18,19] The negative potential on the cathode forms an interfacial electric field that attracts cations from the electrolyte to the cathode outer Helmholtz plane.[20] At steady-state conditions, potassium and carbonate ions are present in excess of the solubility limit, resulting in the formation of solid

potassium carbonate salts. This effect is not expected to be unique to potassium carbonate; carbonates of other commonly used alkali metal cations will have more salt formation issues due to their lower solubility limits (Table S1).[21] These salts precipitate within the catalyst and gas diffusion layers, progressively reducing CO_2 mass transport until the pores are completely blocked and CO_2RR is eliminated. Salt precipitation—inevitable at steady-state conditions—precludes stable CO_2RR.

The conventional approach to mitigate the effects of carbonate salt formation has been to rinse the electrode with water, either by disassembling the cell or injecting water periodically into the CO_2 supply during operation.[22,23] The addition of water content hampers CO_2 transport to the catalyst layer, thereby encouraging hydrogen (H_2) generation and lowering CO_2 electrolysis efficiency during and immedi-
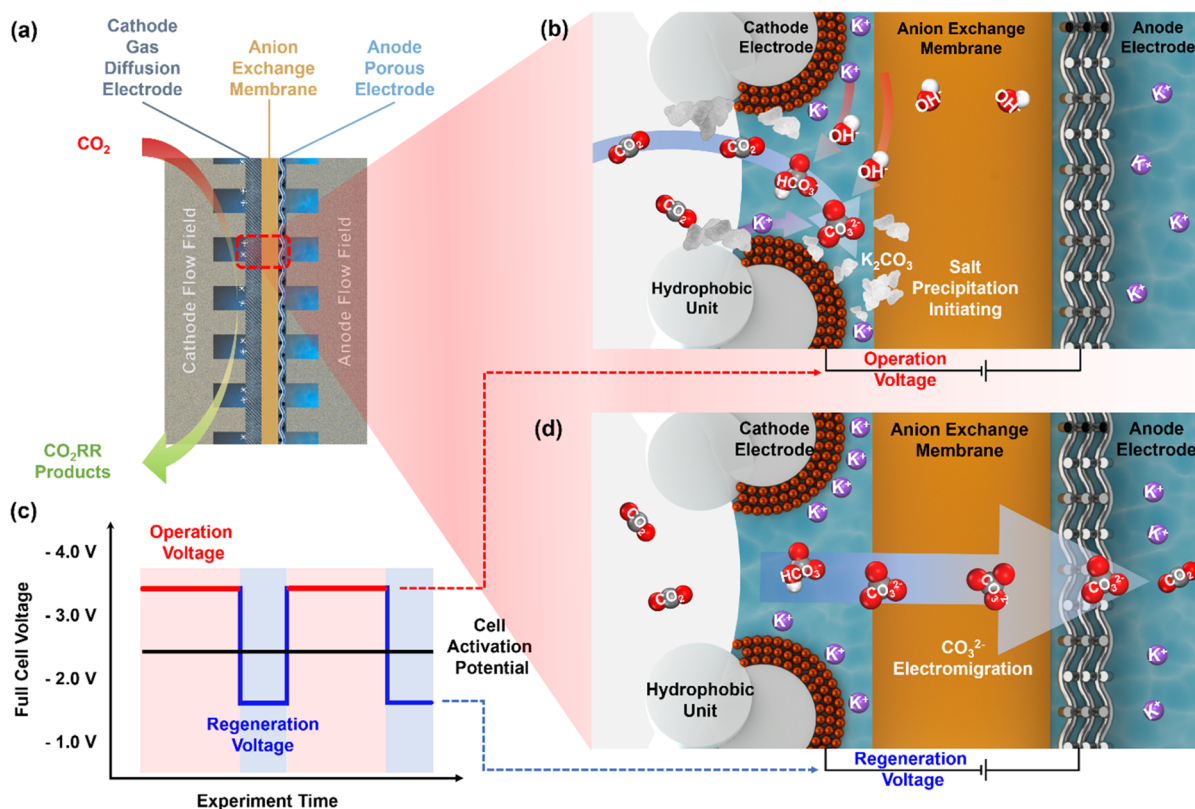
Figure 1. Carbonate formation in MEA CO_2 electrolyzers and the self-cleaning CO_2 reduction strategy. (a) Schematic of the MEA CO_2 electrolyzer. (b) CO_2 conversion to bicarbonate and carbonate during regular electrolyzer operation. (c) Strategy to mitigate carbonate formation by cycling between operational and regeneration cell voltages. (d) Carbonate migration during cell operation at the regeneration voltage.

ately after the washing cycle. Systems using rinsing-based approaches have achieved only small enhancements in stability (<10 h total duration) and struggle to maintain a stable current density.[23−25] Salt precipitation occurs deep in the microporous layer of the gas diffusion electrode and once formed is very difficult to remove.

In this work, we sought to prevent salt formation by alternating our applied cell voltage between an operational voltage and a lower regeneration voltage (Figure 1c). Different alternating voltage and pulsed electrolysis strategies have been employed in CO_2 electrolyzers with a range of duty cycles.[26] Depending on the specific conditions, previous reports have been able to adjust the surface $CO:H_2$ ratio,[27] increase C_{2+} production,[28] and decrease H_2 generation.[29] Our computational modeling illustrates that steady-state operation of CO_2 electrolyzers yields high carbonate concentrations which lead to inevitable salt formation. To avoid these steady-state conditions, we employ a regeneration potential that lowers the reaction rate to nearly 0 mA cm^{-2}, eliminating hydroxide formation, while maintaining a sufficiently negative polarization at the cathode to transport carbonate ions to the anode under electromigration (Figure 1d). Using carbon paper and PTFE-based electrodes for silver and copper catalysts, respectively, we perform CO_2 electrolysis in an MEA. This alternating voltage approach produces a product distribution similar to that of the constant voltage operation but demonstrates much better stability, 157 h of operation (236 h of total duration) as compared to ∼10 h when copper−PTFE electrodes were operated continuously.

To better understand this salt prevention strategy, a computational model of CO_2RR was developed to assess the concentration profiles of key species during operation (Figure S1). When we operated at a constant voltage of −3.8 V, the local carbonate concentration reached the potassium carbonate solubility limit (the solubility product constant = 2073 at 20 °C, Supporting Information Solubility Calculation)[30] within 1200 s (Figure 2a). Salt crystal formation is expected where the computational model predicts salt ions in excess of the solubility limit (indicated in Figure 2). Steady-state conditions were reached after 4000 s with the local potassium and carbonate ionic concentration on the cathode well above the solubility limit. These results confirmed that steady-state conditions cannot be achieved without the local concentration of carbonate exceeding saturation, and thus, salt precipitation is inherent and inevitable in these systems on the time scale of minutes. However, after the first 60 s of operation, the carbonate concentration was only 2.1 M, well below the potassium carbonate solubility limit.

We then simulated various regeneration periods at −2.0 V to analyze concentration changes immediately after 60 s of operation (Figure 2b). This cell voltage was the highest voltage which could obtain a near-zero current density (below 1 mA cm^{-2} on average, Figure S2), thereby maximizing the electric field strength and minimizing hydroxide/carbonate generation. The results demonstrate that increasing the regeneration time significantly reduced the carbonate concentration at the cathode. Applying a 30 s regeneration period lowered the carbonate concentration ∼2000-fold, to ∼10^{-3} M from its preregeneration level of 2.1 M, indicating an elimination of
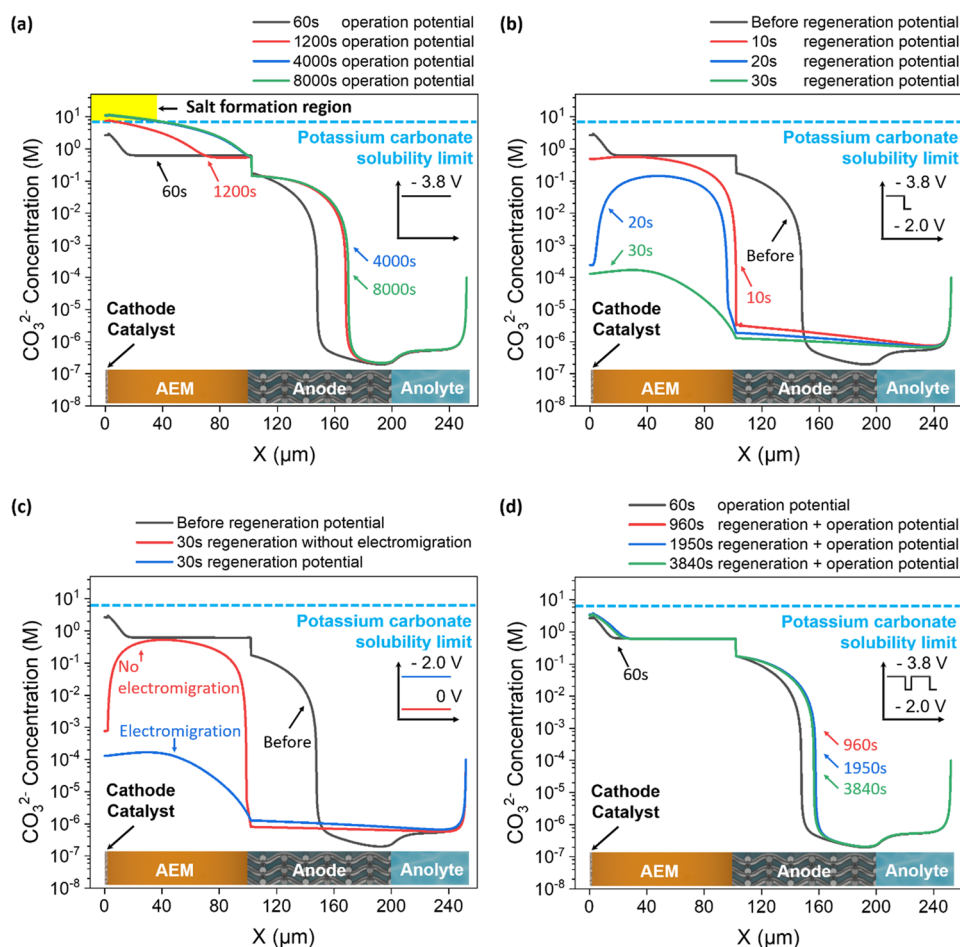
Figure 2. Carbonate concentrations within the MEA: (a) different operational times for continuous operation at −3.8 V (current density of 172 mA cm^{-2}), (b) different regeneration times (regeneration voltage = −2.0 V) after 60 s of continuous operation, (c) comparison of electromigrative and concentration-driven diffusive effects, and (d) different total times when applying the alternating voltage strategy (periodic 60 s of operational voltage and 30 s of regeneration voltage). Salt crystal formation is predicted where salt concentrations in the model exceed the solubility limit (indicated by the dashed line).

>99.9% of carbonate at the cathode. During the operational period carbonates still travel to the anode, but the rate of generation exceeds the migration rate (Figure S3). To verify that electromigration, not thermodynamic diffusion, was responsible for these lower carbonate concentrations, we temporarily removed electromigrative effects from the model. Without electromigration, the carbonate concentrations in the cathode catalyst layer were at least an order of magnitude higher (Figure 2c) and the hydroxide concentrations were also substantially higher (Figure S4). These findings suggest that a regeneration step can maintain carbonate concentrations below the solubility limit and thereby prevent salt formation.

To showcase the promise of this alternating strategy, we simulated a cycle with 60 s operation followed by 30 s regeneration (Figure 2c). The highest carbonate concentration reached in the alternating simulation was 3.4 M, well below the solubility limit. This limit was reached at ∼2000 s (22 periods) after which the peak species concentrations did not increase further with the highest carbonate concentration reaching only 3.4 M at this time. Simulations were also performed with shorter regeneration times per cycle, namely, 10 and 20 s variants, but the peak carbonate concentrations were much closer to the solubility limit (e.g., the 20 s regeneration time had a peak carbonate concentration of ∼6 M, Figure S5). Although hydroxide and bicarbonate ions can also form salt

precipitates with potassium cations, the peak concentrations of these ions in our models are much lower than their respective solubility limits, suggesting that carbonate is the dominant salt precipitate in this system (Figure S1). The alternating voltage strategy maintains a stable carbonate concentration below the carbonate salt solubility limit.

To demonstrate our carbonate reduction strategy, we fabricated a cathode by spraying a carbon gas diffusion layer with silver nanoparticles to produce carbon monoxide (CO) in a CO$_2$RR MEA electrolyzer. 0.1 M potassium bicarbonate was used as anolyte, and an iridium-based catalyst was used to perform oxygen evolution (Supporting Information, Sample Preparation). Performing CO$_2$RR at a constant operational voltage of −3.6 V, after just 12 h of operation, the CO selectivity dropped from 98% to 76% (Figure 3a). During that operational period, the H$_2$ selectivity increased by a complementary amount, while the current density decreased slightly from 170 to 160 mA cm^{-2}. This behavior is typical, characteristic of salt formation in the reactor and associated blockage of reactant CO$_2$ (see inset of Figure 3a).

Applying the unsteady electrochemical forcing strategy, we cycled the system with 60 s at the same operational voltage (−3.6 V) with 30 s of regeneration at −2.0 V (Figure 3b). For a direct comparison with the continuous test, this alternating system was operated for 12 h (18 h total duration). Unlike the
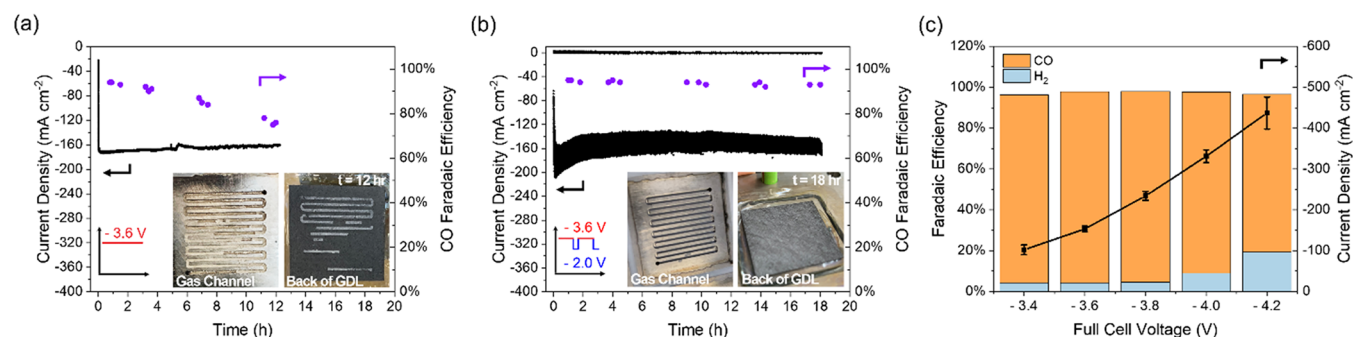
Figure 3. Electrochemical performance of silver catalyst on carbon paper: (a) stability of continuously operated sample at −3.6 V, (b) stability of alternating operation sample (60 s at operational voltage and 30 s at regeneration voltage of −2.0 V), and (c) selectivity of alternating operation sample at different operational voltages.
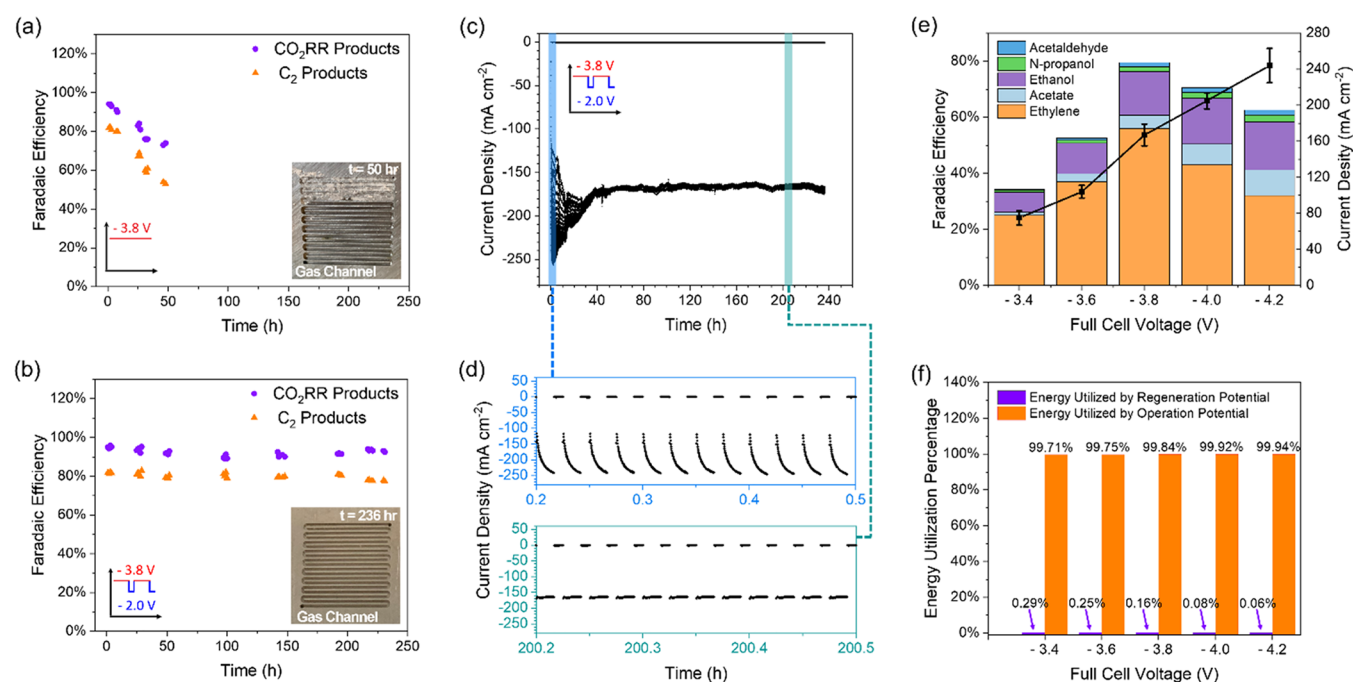

Figure 4. Electrochemical performance of copper catalyst on PTFE electrode: (a) selectivity of continuously operated sample at −3.8 V during long-term operation, (b) selectivity of alternating operation sample (60 s at operational voltage of −3.8 V and 30 s at regeneration voltage of −2.0 V) during long-term operation, (c) current density of alternating operation sample during long-term operation, (d) magnified early view of current density and late view of current density, (e) selectivity of alternating operation sample at different operational voltages, and (f) energy expended on regeneration and operational modes.

continuously operated reactor, which operated at the same current density for the same amount of operational time, this reactor had no visible salt formation and sustained a high CO selectivity. Upon comparison of operational voltages over short time scales, the alternating sample (Figure 3c and Table S2) exhibited selectivities and current densities similar to those of the sample operated continuously (Figure S6). The test was stopped after 18 h (total) for direct comparison with the continuously operated system.

To ensure that the stability improvements of the alternating strategy were from the regeneration period and not from the lower average current density, we operated a silver cathode sample at a slightly lower constant operational voltage (−3.4 V shown in Figure S7). After 18 h of continuous operation the effects of salt precipitation were again major; the CO selectivity had decreased to 83%, and salt precipitates half-filled the gas channels. With the same time-averaged current and total

charge passed, the alternating strategy yielded stable performance and no detectable carbonate salt.

To demonstrate the versatility of our strategy, we applied it to a copper-based catalyst on a PTFE-based electrode design reported previously (Supporting Information, Sample Preparation).[13,31] Despite the change in both the catalyst material and electrode substrate, the stability was maintained. When the copper electrode was operated continuously, there was much salt precipitation visible after 48 h (Figure S8), which in turn caused the CO_2RR selectivity to decrease to 72% (Figure 4a) and the current density to decline (Figure S9). Raman analysis of the cathode salt precipitates confirmed potassium carbonate to be the dominant precipitate (Figure S10). Operating a silver sample on PTFE yielded similar salt precipitation, confirming that CO_2RR products were not the cause of precipitation on these PTFE electrodes (Figure S11). Unsteady forcing, with 60 s of operation at −3.8 V followed by 30 s of regeneration at −2.0 V, yielded a stable CO_2RR selectivity for 157 operational

hours (236 h of total duration) with no detectable evidence of salt formation (Figure S12) and no degradation in performance prior to shutting down the experiment (Figure 4b).

The current density of the copper–PTFE system fluctuated during the 236 h experiment (Figure 4c). Early in the experiment, there was a gradual increase in current density from 110 to 250 mA cm^{-2} during the 60 s of operation, as the electrolyzer cycled back to the operational voltage (Figure 4d). However, after 2000 cycles (50 h total duration), the response of the current density was immediate upon application of the operational voltage, jumping to 175 mA cm^{-2} and remaining constant for the 60 s operational period (Figure 4d). This change in temporal response suggests that the capacitance of the system decreased during the run such that the electrical double layer responded quickly to the application of the higher voltage. In battery and water electrolyzer applications, a similar decay in capacitance is observed for copper- and iridum-based catalysts when cycled over long periods.[32−34] After this initial warm-up period, the alternating system achieved a fast current response to the voltage change to maintain a uniform reaction rate during the operational periods. *Ex situ* XPS analysis of a copper sample suggests that the catalyst was in metallic form during operation (Figure S13).

The current density and product selectivity were nearly identical for the alternating (Figure 4e and Table S2) and continuous (Figure S14) operational forms over short time scales at different operational voltages. To the best of our knowledge, the stability toward C_2 products reported here is the longest in current literature among CO_2 electrolyzers operating at industrially viable currents (Table S3). Because the regeneration voltage was selected to be well below the activation voltage, the regeneration period operates at a negligible current, much lower current than the operational period. Therefore, there is minimal additional energy required to power the regeneration period because the regeneration period consumes less than 1% of the system energy requirements (Figure 4f). The alternating system also minimizes the addition of new electrolyte salts, new catalyst materials, and catalyst replacement downtimes, combining for a significant operational advantage.

In summary, when CO_2 electrolysis is performed at industrially relevant current densities, the steady-state alkaline conditions lead, inevitably, to salt formation. We presented a self-cleaning CO_2 reduction strategy to circumvent the steady state by cycling between an operational and regeneration voltage. The regeneration period maintained an electric field for carbonate ions to migrate to the anode, lowered cathode concentrations, and avoided damaging salt formation. This approach was applied to silver and copper catalysts on carbon paper and PTFE-based electrodes, respectively. The product selectivity of the alternating mode was shown to be similar to that of the continuous operation, with the advantage that alternating operation yielded no detectable carbonate formation, thereby enabling long-term stable operation. The loss of reactant CO_2 to carbonates is a larger challenge before the field; the strategy presented here avoids the associated damage to the cell that has limited the stability—and applicability—of CO_2RR systems. Using this strategy, we were able to operate a copper–PTFE sample in an MEA-based electrolyzer for 157 h (236 h total duration), maintaining a C_2 product selectivity of 80% and a C_2 partial current density of 138 mA cm^{-2} with a cost of <1% additional system energy input.

■ ASSOCIATED CONTENT

ⓢ Supporting Information

The Supporting Information is available free of charge at https://pubs.acs.org/doi/10.1021/acsenergylett.0c02401.

> COMSOL Multiphysics simulation results and model mechanism; current density plots of the different regeneration voltages; current density and selectivity plots of continuous operation of silver and copper catalysts; electrochemical performance comparison between continuous and alternating voltage with the same average current density; current density and selectivity of continuous operation of silver catalyst; electrode preparation; operation of the electrochemical MEA cell; product analysis (PDF)

■ AUTHOR INFORMATION

Corresponding Authors

Edward H. Sargent − *Department of Electrical and Computer Engineering, University of Toronto, Toronto, Ontario M5S 3G4, Canada;* ⊙ orcid.org/0000-0003-0396-6495; Email: ted.sargent@utoronto.ca

David Sinton − *Department of Mechanical and Industrial Engineering, University of Toronto, Toronto, Ontario M5S 3G8, Canada;* ⊙ orcid.org/0000-0003-2714-6408; Email: sinton@mie.utoronto.ca

Authors

Yi Xu − *Department of Mechanical and Industrial Engineering, University of Toronto, Toronto, Ontario M5S 3G8, Canada;* ⊙ orcid.org/0000-0002-8108-0975

Jonathan P. Edwards − *Department of Mechanical and Industrial Engineering, University of Toronto, Toronto, Ontario M5S 3G8, Canada;* ⊙ orcid.org/0000-0003-4000-5802

Shijie Liu − *Department of Mechanical and Industrial Engineering, University of Toronto, Toronto, Ontario M5S 3G8, Canada;* ⊙ orcid.org/0000-0003-1947-6001

Rui Kai Miao − *Department of Mechanical and Industrial Engineering, University of Toronto, Toronto, Ontario M5S 3G8, Canada;* ⊙ orcid.org/0000-0002-0542-0683

Jianan Erick Huang − *Department of Electrical and Computer Engineering, University of Toronto, Toronto, Ontario M5S 3G4, Canada*

Christine M. Gabardo − *Department of Mechanical and Industrial Engineering, University of Toronto, Toronto, Ontario M5S 3G8, Canada;* ⊙ orcid.org/0000-0002-9456-6894

Colin P. O'Brien − *Department of Mechanical and Industrial Engineering, University of Toronto, Toronto, Ontario M5S 3G8, Canada;* ⊙ orcid.org/0000-0003-0824-2752

Jun Li − *Department of Mechanical and Industrial Engineering and Department of Electrical and Computer Engineering, University of Toronto, Toronto, Ontario M5S 3G8, Canada;* ⊙ orcid.org/0000-0002-1958-5665

Complete contact information is available at:
https://pubs.acs.org/10.1021/acsenergylett.0c02401

Notes

The authors declare the following competing financial interest(s): There is a patent application pending, filed by the authors of this Letter and their institutions.

ACKNOWLEDGMENTS

REFERENCES

(1) Hepburn, C.; Adlen, E.; Beddington, J.; Carter, E. A.; Fuss, S.; Mac Dowell, N.; Minx, J. C.; Smith, P.; Williams, C. K. The Technological and Economic Prospects for CO2 Utilization and Removal. *Nature* **2019**, *575* (7781), 87−97.

(2) Burney, J. A. The Downstream Air Pollution Impacts of the Transition from Coal to Natural Gas in the United States. *Nat. Sustain.* **2020**, *3* (2), 152−160.

(3) International Renewable Energy Agency. *IRENA: Renewable Power Generation Costs in 2017*; 2018.

(4) Bushuyev, O. S.; De Luna, P.; Dinh, C. T.; Tao, L.; Saur, G.; van de Lagemaat, J.; Kelley, S. O.; Sargent, E. H. What Should We Make with CO2and How Can We Make It? *Joule* **2018**, *2* (5), 825−832.

(5) Jouny, M.; Luc, W.; Jiao, F. General Techno-Economic Analysis of CO 2 Electrolysis Systems. *Ind. Eng. Chem. Res.* **2018**, *57* (6), 2165−2177.

(6) Barnhart, C. J.; Dale, M.; Brandt, A. R.; Benson, S. M. The Energetic Implications of Curtailing versus Storing Solar- and Wind-Generated Electricity. *Energy Environ. Sci.* **2013**, *6* (10), 2804.

(7) Saadi, F. H.; Lewis, N. S.; McFarland, E. W. Relative Costs of Transporting Electrical and Chemical Energy. *Energy Environ. Sci.* **2018**, *11* (3), 469−475.

(8) Edwards, J. P.; Xu, Y.; Gabardo, C. M.; Dinh, C.-T.; Li, J.; Qi, Z.; Ozden, A.; Sargent, E. H.; Sinton, D. Efficient Electrocatalytic Conversion of Carbon Dioxide in a Low-Resistance Pressurized Alkaline Electrolyzer. *Appl. Energy* **2020**, *261*, 114305.

(9) Jiang, K.; Huang, Y.; Zeng, G.; Toma, F. M.; Goddard, W. A.; Bell, A. T. Effects of Surface Roughness on the Electrochemical Reduction of CO2 over Cu. *ACS Energy Lett.* **2020**, *5* (4), 1206−1214.

(10) Salvatore, D. A.; Weekes, D. M.; He, J.; Dettelbach, K. E.; Li, Y. C.; Mallouk, T. E.; Berlinguette, C. P. Electrolysis of Gaseous CO2 to CO in a Flow Cell with a Bipolar Membrane. *ACS Energy Lett.* **2018**, *3* (1), 149−154.

(11) Xu, Y.; Edwards, J. P.; Zhong, J.; O'Brien, C. P.; Gabardo, C. M.; McCallum, C.; Li, J.; Dinh, C.-T.; Sargent, E. H.; Sinton, D. Oxygen-Tolerant Electroproduction of C 2 Products from Simulated Flue Gas. *Energy Environ. Sci.* **2020**, *13* (2), 554−561.

(12) Kung, C. W.; Audu, C. O.; Peters, A. W.; Noh, H.; Farha, O. K.; Hupp, J. T. Copper Nanoparticles Installed in Metal-Organic Framework Thin Films Are Electrocatalytically Competent for CO2 Reduction. *ACS Energy Lett.* **2017**, *2* (10), 2394−2401.

(13) Gabardo, C. M.; O'Brien, C. P.; Edwards, J. P.; McCallum, C.; Xu, Y.; Dinh, C.-T.; Li, J.; Sargent, E. H.; Sinton, D. Continuous Carbon Dioxide Electroreduction to Concentrated Multi-Carbon Products Using a Membrane Electrode Assembly. *Joule* **2019**, *3* (11), 2777−2791.

(14) Jouny, M.; Luc, W.; Jiao, F. General Techno-Economic Analysis of CO2 Electrolysis Systems. *Ind. Eng. Chem. Res.* **2018**, *57* (6), 2165−2177.

(15) Verma, S.; Kim, B.; Jhong, H.-R.; Ma, S.; Kenis, P. J. A. A Gross-Margin Model for Defining Technoeconomic Benchmarks in the Electroreduction of CO2. *ChemSusChem* **2016**, *9* (15), 1972−1979.

(16) Ringe, S.; Clark, E. L.; Resasco, J.; Walton, A.; Seger, B.; Bell, A. T.; Chan, K. Understanding Cation Effects in Electrochemical CO 2 Reduction. *Energy Environ. Sci.* **2019**, *12* (10), 3001−3014.

(17) Resasco, J.; Chen, L. D.; Clark, E.; Tsai, C.; Hahn, C.; Jaramillo, T. F.; Chan, K.; Bell, A. T. Promoter Effects of Alkali Metal Cations on the Electrochemical Reduction of Carbon Dioxide. *J. Am. Chem. Soc.* **2017**, *139* (32), 11277−11287.

(18) Lu, X.; Zhu, C.; Wu, Z.; Xuan, J.; Francisco, J. S.; Wang, H. In Situ Observation of the PH Gradient near the Gas Diffusion Electrode of CO 2 Reduction in Alkaline Electrolyte. *J. Am. Chem. Soc.* **2020**, *142* (36), 15438−15444.

(19) Zhong, H.; Fujii, K.; Nakano, Y.; Jin, F. Effect of CO 2 Bubbling into Aqueous Solutions Used for Electrochemical Reduction of CO 2 for Energy Conversion and Storage. *J. Phys. Chem. C* **2015**, *119* (1), 55−61.

(20) Singh, M. R.; Kwon, Y.; Lum, Y.; Ager, J. W.; Bell, A. T. Hydrolysis of Electrolyte Cations Enhances the Electrochemical Reduction of CO2 over Ag and Cu. *J. Am. Chem. Soc.* **2016**, *138* (39), 13006−13012.

(21) Kibria, M. G.; Edwards, J. P.; Gabardo, C. M.; Dinh, C.; Seifitokaldani, A.; Sinton, D.; Sargent, E. H. Electrochemical CO 2 Reduction into Chemical Feedstocks: From Mechanistic Electrocatalysis Models to System Design. *Adv. Mater.* **2019**, *31* (31), 1807166.

(22) Nwabara, U. O.; Cofell, E. R.; Verma, S.; Negro, E.; Kenis, P. J. A. Durable Cathodes and Electrolyzers for the Efficient Aqueous Electrochemical Reduction of CO 2. *ChemSusChem* **2020**, *13* (5), 855−875.

(23) Verma, S.; Hamasaki, Y.; Kim, C.; Huang, W.; Lu, S.; Jhong, H.-R. M.; Gewirth, A. A.; Fujigaya, T.; Nakashima, N.; Kenis, P. J. A. Insights into the Low Overpotential Electroreduction of CO2 to CO on a Supported Gold Catalyst in an Alkaline Flow Electrolyzer. *ACS Energy Lett.* **2018**, *3* (1), 193−198.

(24) Endrödi, B.; Kecsenovity, E.; Samu, A.; Darvas, F.; Jones, R. V.; Török, V.; Danyi, A.; Janáky, C. Multilayer Electrolyzer Stack Converts Carbon Dioxide to Gas Products at High Pressure with High Efficiency. *ACS Energy Lett.* **2019**, *4* (7), 1770−1777.

(25) De Mot, B.; Ramdin, M.; Hereijgers, J.; Vlugt, T. J. H.; Breugelmans, T. Direct Water Injection in Catholyte-Free Zero-Gap Carbon Dioxide Electrolyzers. *ChemElectroChem* **2020**, *7* (18), 3839−3843.

(26) Kim, C.; Weng, L.-C.; Bell, A. T. Impact of Pulsed Electrochemical Reduction of CO 2 on the Formation of C 2+ Products over Cu. *ACS Catal.* **2020**, *10* (21), 12403−12413.

(27) Kumar, B.; Brian, J. P.; Atla, V.; Kumari, S.; Bertram, K. A.; White, R. T.; Spurgeon, J. M. Controlling the Product Syngas H 2:CO Ratio through Pulsed-Bias Electrochemical Reduction of CO 2 on Copper. *ACS Catal.* **2016**, *6* (7), 4739−4745.

(28) Arán-Ais, R. M.; Scholten, F.; Kunze, S.; Rizo, R.; Roldan Cuenya, B. The Role of in Situ Generated Morphological Motifs and Cu(i) Species in C2+ Product Selectivity during CO2 Pulsed Electroreduction. *Nat. Energy* **2020**, *5* (4), 317−325.

(29) Kimura, K. W.; Fritz, K. E.; Kim, J.; Suntivich, J.; Abruña, H. D.; Hanrath, T. Controlled Selectivity of CO 2 Reduction on Copper by Pulsing the Electrochemical Potential. *ChemSusChem* **2018**, *11* (11), 1781−1786.

(30) CRC Handbook of Chemistry and Physics: A Ready-Reference Book of Chemical and Physical Data. *Choice Rev. Online* 2010 *47* (07) 47-3553. DOI: 10.5860/CHOICE.47-3553.

(31) Dinh, C.-T.; Burdyny, T.; Kibria, M. G.; Seifitokaldani, A.; Gabardo, C. M.; García de Arquer, F. P.; Kiani, A.; Edwards, J. P.; De Luna, P.; Bushuyev, O. S.; Zou, C.; Quintero-Bermudez, R.; Pang, Y.; Sinton, D.; Sargent, E. H. CO 2 Electroreduction to Ethylene via Hydroxide-Mediated Copper Catalysis at an Abrupt Interface. *Science (Washington, DC, U. S.)* **2018**, *360* (6390), 783−787.

(32) Lai, C. M.; Kao, T. L.; Tuan, H. Y. Si Nanowires/Cu Nanowires Bilayer Fabric as a Lithium Ion Capacitor Anode with Excellent Performance. *J. Power Sources* **2018**, *379*, 261−269.

(33) Hsu, Y.-K.; Chen, Y.-C.; Lin, Y.-G. Synthesis of Copper Sulfide Nanowire Arrays for High-Performance Supercapacitors. *Electrochim. Acta* **2014**, *139*, 401−407.

(34) Malleo, D.; Nevill, J. T.; van Ooyen, A.; Schnakenberg, U.; Lee, L. P.; Morgan, H. Note: Characterization of Electrode Materials for Dielectric Spectroscopy. *Rev. Sci. Instrum.* **2010**, *81* (1), 016104.